# THE STUDENT DUST COUNTER ON THE NEW HORIZONS MISSION

M. HORÁNYI, V. HOXIE, D. JAMES[#], A. POPPE[#], C. BRYANT[#], B. GROGAN[*], B. LAMPRECHT, J. MACK, F. BAGENAL, S. BATISTE, N. BUNCH[*], T. CHANTHAWANICH[*], F. CHRISTENSEN[*], M. COLGAN[*], T. DUNN[*], G. DRAKE, A. FERNANDEZ[#], T. FINLEY[#], G. HOLLAND[#], A. JENKINS[*], C. KRAUSS[#], E. KRAUSS[*], O. KRAUSS[*], M. LANKTON, C. MITCHELL[#], M. NEELAND[*], T. REESE, K. RASH[*], G. TATE, C. VAUDRIN[*], J. WESTFALL

*Laboratory for Atmospheric and Space Physics, University of Colorado, Boulder, CO, 80309-0392, USA* (`mihaly.horanyi@colorado.edu`)
[*] *undergraduate student*
[#] *graduate student*

**Abstract.** The Student Dust Counter (SDC) experiment of the New Horizons Mission is an impact dust detector to map the spatial and size distribution of dust along the trajectory of the spacecraft across the solar system. The sensors are thin, permanently polarized polyvinylidene fluoride (PVDF) plastic films that generate an electrical signal when dust particles penetrate their surface. SDC is capable of detecting particles with masses $m > 10^{-12}$ g, and it has a total sensitive surface area of about 0.1 m$^2$, pointing most of the time close to the ram direction of the spacecraft. SDC is part of the Education and Public Outreach (EPO) effort of this mission. The instrument was designed, built, tested, integrated, and now is operated by students.

## 1. Introduction

The Student Dust Counter (SDC) is an impact dust detector on board the New Horizons Mission. It is designed to map the spatial and size distribution of interplanetary dust particles in order to verify the existence of the predicted structures in our dust disk, the Zodiacal cloud. Five spacecraft have carried dust detectors beyond the asteroid belt: Pioneers 10 and 11 (Humes, 1980), Ulysses, Galileo (Grün *et al.*, 1993), and Cassini (Srama *et al.*, 2004). SDC will provide the first dust measurements beyond 18 AU, where the Pioneer sensors stopped working. After the Pluto-Charon fly-by, SDC will continue to measure dust on into the Kuiper Belt. These observations will advance our understanding of the origin and evolution of our own solar system, and allow for comparative studies of planet formation in dust disks around other stars.

SDC is part of the Education and Public Outreach (EPO) effort of the New Horizons mission and is the first science instrument on a planetary mission to be designed, built, tested and operated by students. The SDC project has an unusual history. A similar professional dust instrument was part of a competing proposal to New Horizons in a parallel Phase A study. After the selection of New Horizons, motivated by the potential scientific contribution of a dust instrument, the idea emerged to redirect some of the funds from traditional EPO activities, and to involve a group of students to try their hands on building space hardware. The advanced state of the rest of the New Horizons payload, and the risk of involving unexperienced students made this request difficult. With the strong support of the mission PI, the NASA EPO board agreed to try the 'SDC experiment'.

To minimize the risk SDC might pose to the mission, all quality assurance inspections and the final flight assembly was done by NASA certified personnel, and student activities were supervised by professionals. However, the student team, consisting of up to 20 engineering and physics undergraduate and graduate students, was responsible for the work done in all phases of this project, including presentations at all NASA milestone reviews. SDC was built and tested to the same NASA engineering standards as every other flight instrument. Due to the long duration of the New Horizons mission, generations of future students will continue to be involved, handing over their skills to the groups that follow them.

After 6 months of successful operations in space the SDC instrument was renamed, and the dedication reads:

*New Horizons, the first mission to Pluto and the Kuiper Belt, is proud to announce that the student instrument (SDC) aboard our spacecraft is hereby named "The Venetia Burney Student Dust Counter" in honor of Ms. Venetia Burney Phair, who at age of eleven nominated the name Pluto for our solar system's ninth planet. May "Venetia" inspire a new generation of students to explore our solar system, to make discoveries which challenge the imagination, and to pursue learning all through their lives.*

## 2.  Science background

The interplanetary dust particle (IDP) population reflects a complex balance between sources, transport, and sinks which are all functions of the dust particle sizes and their positions in the solar system. IDPs are created primarily in asteroid-asteroid collisions, from the disintegration of comets near the Sun, from collisions between Kuiper Belt objects (KBOs), and the continuous meteoroid bombardment of the moons, rings, asteroids and KBOs. Data from near-Earth and deep space missions suggest five distinct

IDP populations (Divine, 1993). While this model makes predictions for IDP populations throughout the solar system, it has not been validated by direct measurements beyond 18 AU.

Beginning at about 3 AU from the Sun, the Pioneer 10 and 11 observations of particles larger than about 10 $\mu$m in radius showed a constant spatial density (number of particles per unit volume) out to 18 AU (Humes, 1980). At this distance, the argon and nitrogen gas mixture in the Pioneer pressurized detector cells froze and no further measurements could be made.

IDPs born on the outskirts of the solar system slowly lose orbital energy due to Poynting-Robertson drag and migrate toward the Sun. A 10 $\mu$m radius grain born at 50 AU reaches the inner solar system in about 6.5 My. However, the continuous migration can significantly slow down or come to a halt due to mean motion resonances with the planets (Liou and Zook, 1999; Martin and Malhotra, 2002; Martin and Malhotra, 2003). Grains can also get ejected from the solar system via close encounters with the planets (Liou *et al.*, 1996). Orbital integrations find that Neptune prolongs the lifetime of the inwardly migrating dust grains outside its orbit, imprinting its resonance structure on the spatial density of dust in the Kuiper Belt.

Jupiter, on the other hand, acts as a gate-keeper and keeps the inner part of our solar system relatively dust free by ejecting up to 80% of the particles that would cross its orbit. The nature of the inner planets effect on dust distribution is largely hidden due to dust production from active comets.

SDC measurements made as New Horizons crosses the solar system will help to understand the generation, the transport, and the loss processes of IDPs. The measurements of the density variations outside the orbit of Jupiter will allow for estimating the rate of dust production in the Kuiper Belt, the collisional history of the region, and the mass distribution of the primordial KBO population (Stern, 1996).

## 3. Instrument description

The SDC instrument (Figure 1) consists of a set of polyvinylidene fluoride (PVDF) film impact sensors, carried on a detector support panel, which is mounted on the exterior of the New Horizons spacecraft. It is outside the spacecraft multi-layer insulating (MLI) blanket, facing the ram direction. Signals from the sensors are collected through an intra-harness that runs from the detector assembly into the spacecraft interior to the instrument electronics box mounted opposite the detector panel.

The measurement requirements of the SDC instrument were established by estimating the particle mass detection limit needed to resolve the expected features of the dust distribution. The characteristic width of the predicted resonance structures is on the order of 1 AU, hence a spatial
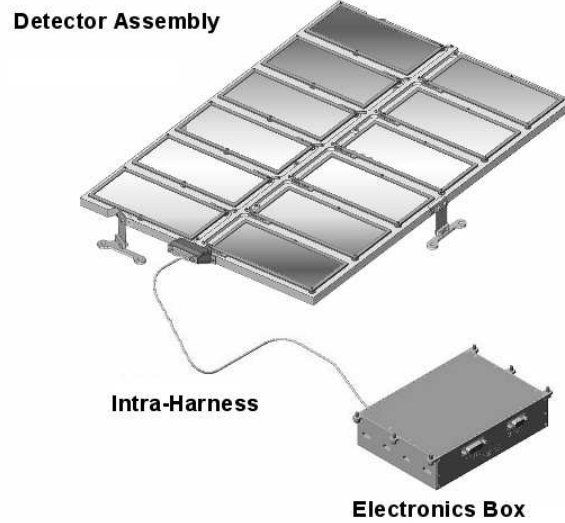
**Detector Assembly**

**Intra-Harness**

**Electronics Box**

*Figure 1.* The Student Dust Counter provides $\sim 0.1$ m$^2$ of sensitive area. It was designed to measure the mass of IDPs in the range of $10^{-12}$ to $10^{-9}$ g. It continues registering the impacts of bigger dust particles without the ability to determine their mass. It weighs 1.6 kg and consumes 5.1 watts of average power.

resolution of $\approx 0.1$ AU assures adequate sampling. With the characteristic spacecraft speed, during cruise, of $\approx 13$ km/s, this is equivalent to an integration period of one week. Based on the current models (Divine, 1993) outside of dust structures, a detector, with a lower mass detection limit of about $10^{-12}$ g and 0.1 m$^2$ surface area, is predicted to have on the order of 1 IDP hit per week. SDC was designed to resolve the mass of IDPs in the range of $10^{-12} < m < 10^{-9}$ g within factors of $< 2$, covering an approximate size range of $1 - 10$ $\mu$m in particle radius. Bigger grains are also recorded without the ability of resolving their mass.

### 3.1. SENSOR DESIGN

SDCs dust impact detection is based on the use of permanently polarized PVDF films. An impacting particle causes a depolarization charge when it penetrates the film. PVDF sensors require no bias voltage, they are simple, inexpensive, reliable, electrically and thermally stable, mechanically rugged, radiation resistant, and do not respond to energetic ions or electrons. PVDF dust detectors have been extensively tested and calibrated in laboratory experiments (Simpson *et al.*, 1989a; Simpson *et al.*, 1989b; Simpson and Tuzzolino, 1985; Tuzzolino, 1992; Tuzzolino, 1996) and have an excellent track record in space experiments. PVDF sensors were flown on the VEGA 1 and 2, Stardust, Cassini, and ARGOS missions (Tuzzolino *et al.*, 2001; Tuzzolino *et al.*, 2003; Srama *et al.*, 2004).

### 3.1.1. *PVDF Signal Generation*

The magnitude of the PVDF depolarization charge depends on particle momentum as well as whether the particle penetrates into or through the film (Simpson and Tuzzolino, 1985). SDC uses 28 $\mu$m thick PVDF films which have been shown to stop particles up to $10^{-10}$ g and speeds up to 20 km/s (Simpson and Tuzzolino, 1985). For particles stopped in the film, the number of electrons generated is given by (Simpson and Tuzzolino, 1985)

$$N_e = 3.8 \times 10^{17} m[\text{g}]^{1.3} v[\text{km/s}]^{3.0}, \tag{1}$$

where $m$ is particle mass, in grams, and $v$ is the impacting velocity in km/s. The speed of long-resident dust grains following circular Kepler orbits in the outer solar system is much less than the velocity of the spacecraft, hence we take $v$ in Eq. 1 to be the spacecraft velocity.

For charge sensing amplifiers, the noise floor is proportional to the detector capacitance (Spieler, 2005) which is a function of the detector area, the material permittivity and the thickness ($C = \epsilon_0 \epsilon_r$ A/d). The relative permittivity of PVDF, like many polymers, changes dramatically with temperature varying from $\epsilon_r = 11$ at 25 °C to 2.5 at -120 °C. For a given thickness of PVDF, and a given operating temperature, the required lower limit of detectable impact-induced charge determines the maximum allowable area of a single sensor. From Eq. 1 the SDC mass threshold of $10^{-12}$ g (sub-micron radius) requires a signal threshold of $6 \times 10^6$ $e$. To ensure a false detection rate of less than 1 per month, a signal-to-noise ratio (SNR) greater than 5 is required for an RMS noise level of $\approx 1 \times 10^5$ $e$. Given the characteristics of the charge sensitive amplifier design used (see section 3.3.1) the maximum allowable capacitance per sensor was determined to be $\sim$30 nF for an equivalent area of $\approx$80 cm$^2$.

To achieve a total sensitive area of 0.1 m$^2$ SDC is composed of 12 sensor patches, each 14.2 cm x 6.5 cm, mounted onto the top surface of a support panel. In addition, there are two reference sensor patches mounted on the back side of the detector support panel, protected from any dust impacts. These reference sensors, identical to the top surface sensors, are used to monitor the various background noise levels, from mechanical vibrations or cosmic ray hits of our electronics, for example.

### 3.1.2. *Sensor Construction*

The SDC detectors (Figure 2) are based on similar instruments from the University of Chicago. The PVDF film used by SDC is manufactured with 1000 $\overset{\circ}{A}$ of Al/Ni electrode material on the top and bottom surfaces. The film is bonded between a pair of G-10 fiberglass frames and electrical contact to the PVDF is made through signal wires running around the interior of the frame apertures and bonded to the electrode material with conductive silver
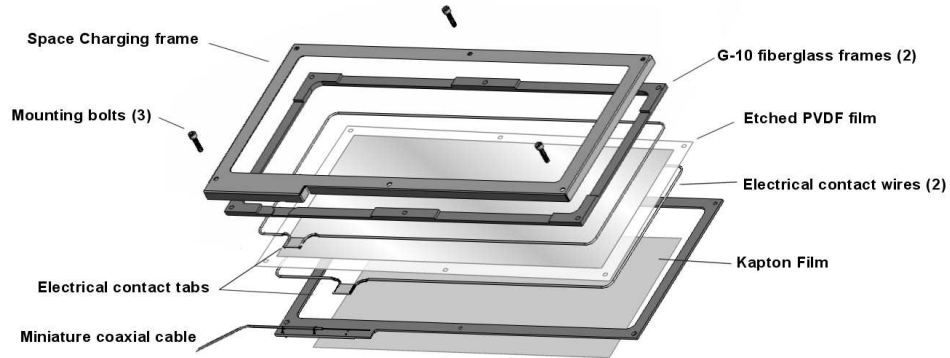
**Space Charging frame**

**Mounting bolts (3)**

**G-10 fiberglass frames (2)**

**Etched PVDF film**

**Electrical contact wires (2)**

**Kapton Film**

**Electrical contact tabs**

**Miniature coaxial cable**

*Figure 2.* Exploded view of a single SDC PVDF detector. The detector is mechanically bonded with structural epoxy. Electrical connection from the PVDF metalization to the signal wires is through silver filled epoxy. The signal wires are soldered to miniature coaxial cables leading to the system electronics. Three mounting screws tie the space charging frame and the detector to the underlying honeycomb support panel.

filled epoxy. The signal wires are routed to connection tabs where a miniature coaxial cable is attached.

## 3.2. MECHANICAL DESIGN

The detector assembly of SDC is built on a ∼1 cm thick aluminum composite honeycomb panel which provides mounting and support for the dust sensors onto the exterior spacecraft deck. The panel is attached to the spacecraft with a three point compliant mount formed by titanium flexures. The flexures are sized to accommodate the thermal expansion mismatch between the spacecraft deck and detector assembly. Sensor wiring on the detector assembly is routed in a harness channel designed to withstand dust impacts.

### 3.2.1. *Thermal Design*

The thermal design of the SDC detector assembly was driven largely by the requirement that the detector panel be able to maintain passive thermal control while in view of the sun during early mission maneuvers. The PVDF sensor film itself has poor thermo-optical properties, and is prone to overheating when exposed to direct sunlight. PVDF will undergo permanent depolarization at temperatures over 85 °C (Simpson and Tuzzolino, 1985). To maintain the PVDF temperature below a design target of 65°C, a high emissivity polyimide tape is applied to the backside of the PVDF film to radiatively couple it to the honeycomb support panel below. The panel facesheet spreads out the heat from beneath the detectors. The top surface
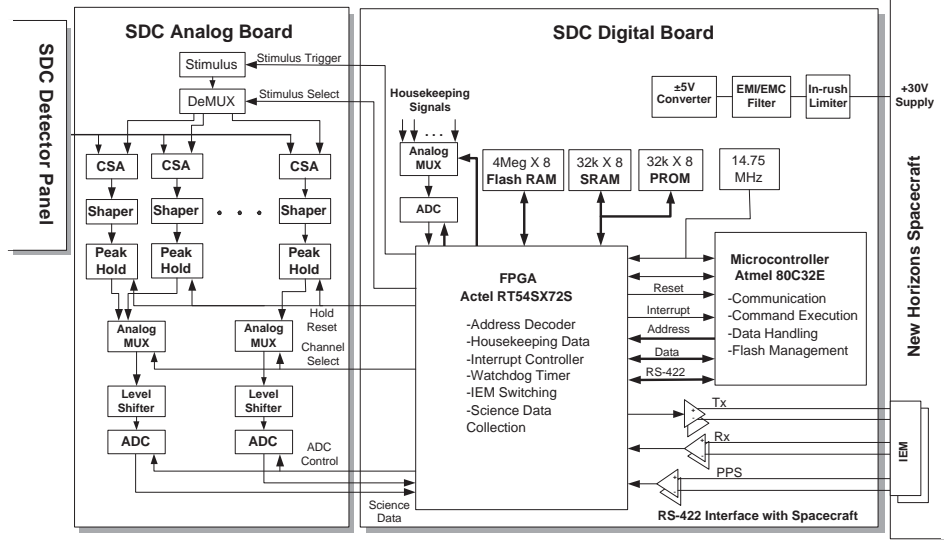
*Figure 3.* SDC Electronics block diagram. Signals from each PVDF detector are routed to individual analog electronics chains. Under FPGA control the science and housekeeping data are collected and passed to the system microprocessor which manages long term storage of data into flash memory. The FPGA also acts as a switch between the redundant spacecraft communications lines and the microprocessor.

is covered with silverized Teflon tape that reflects 90% of the incident solar energy, preventing the panel itself from overheating. The detector support panel area was sized analytically to provide adequate radiating area around the 12 PVDF sensor patches.

## 3.3. Electrical design

The SDC electronics are carried on two multilayer printed wiring assemblies (PWA) housed in the SDC electronics box. Signals from the detectors come through the Intra-harness onto the analog PWA where they are amplified, conditioned and converted to digital data. The digital data is collected to registers in the field programmable gate array (FPGA) on the digital PWA (Figure 3) and from there to the microprocessor which adds time-stamps to the data and stores them in long term non-volatile memory. The digital PWA also contains the power supply, system health monitoring circuitry and interface electronics for spacecraft communications.
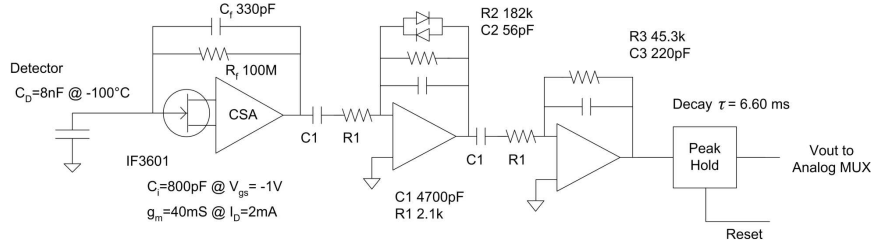
*Figure 4.* Each of the 14 analog signal chains contains a JFET input charge sensitive amplifiers followed by a two stage CR-RC shaper circuit. The first stage shaper includes a logarithmic gain term supporting a $2\times10^5$ to $5\times10^{10}$ electron input range. The shaper output is captured in a peak-hold stage long enough to be sampled by a scanning analog to digital converter circuit.

### 3.3.1. *Analog Signal Chain*

Given the large capacitance of the PVDF detectors, care was taken to simultaneously minimize the noise floor and to maximize the signal-to-noise ratio. Analysis showed that SNR is maximized when detector capacitance is equal to the input capacitance of the charge sensitive amplifier's (CSA) JFET (junction field effect transistor) (Radeka, 1974; Spieler, 2005). To address the problems of matching JFETs to very large capacitance detectors work had previously been done (Bertolaccini *et al.*, 1988) to develop a process that produces high capacitance JFETs with good transconductance.

A by-product of the specific JFET design is an increased gate volume sensitive to energetic particle charge deposition. A CRME96 radiation analysis using the gate dimensions and a critical deposited charge of $1 \times 10^6$ $e$ gives $2.3 \times 10^{-7}$ event s$^{-1}$ during solar max and roughly doubles during solar min. In the nominal case the upset rate is well below the one per month science requirement. Using an ordinary solar flare model with mean composition, the upset rate rises to $1.1 \times 10^{-5}$ event s$^{-1}$, suggesting that higher than expected event rates should be checked against possible space weather effects.

The CSA output is routed to the two stage CR-RC shaper circuit (Figure 4). Using the given CSA design values, theoretical noise limits can be calculated (Spieler, 2005), allowing for the selection of an optimal shaper peaking time $\tau = 10$ $\mu$s. Measured SNR values from prototype circuits agree with the predicted values and show a SNR $> 10$ for $10^6$ electron input signals.

To accommodate signals over the $\approx 4$ orders of magnitude required, the first stage of the shaper includes a logarithmic compression. In order to keep the circuit size small the temperature dependence is uncompensated and must be corrected in post-processing.

Following the shaper section each analog signal chain has a peak hold circuit that retains the shaper pulse maximum for sampling by the analog to digital converters (ADC). The fourteen peak-hold outputs are divided into

two groups of seven with each group routed to its own analog multiplexer (MUX) and 16 bit ADC. A side effect of the signal chain electronics is that low level signals produce a digital output number (DN) of ∼65000 with increasing magnitude analog signals producing decreasing DN values.

The response curve of a representative analog chain through the ADC is shown in Figure 5. The gain shift in the upper size range (lower right of the plot) is from the temperature sensitivity of the diodes in the logarithmic compression term of the first stage shaper. This temperature dependency was characterized during pre-launch calibration (see Section 3.5.2) and the temperatures driving this shift are monitored during flight by temperature sensors on the shaper circuits. Additionally the thermal environment of the SDC electronics box is expected to be stable over long time scales.

### 3.3.2. *On-board Stimulus*
To track changes in the gain of the signal chains during flight the SDC electronics includes stimulus circuitry that can inject selectable charge quantities into any of the signal chains at the JFET gates. The responses to these stimuli are collected in the same manner as science data and reported along with a measurement of the stimulus voltage. The nominal injection levels are shown on Figure 5.

### 3.3.3. *Digital Control Electronics*
The two analog MUX and ADC sets are controlled in parallel by the FPGA on the digital PWA. The ADC conversion values from each channel are stored to registers and compared against individually programmable threshold values in the FPGA. Upon a valid event detection the FPGA executes one additional scan of every channel, to assure the shaper pulse has time to peak, then it stops scanning, leaving each channel's peak value in the FPGA registers. An interrupt is sent to the microprocessor to indicate that the science data is ready. The FPGA provides a control register which can be set to prevent any given channel from generating interrupts.

The system has a radiation tolerant 8032 microcontroller, 32 kbyte anti-fuse PROM for program storage, 32 kbyte rad-hard SRAM and 4 Mbyte non-volatile flash RAM. The data retention time of the flash memory, rated at 10 years, is extended by providing circuitry to power it on only when the system is accessing it. The SDC flight software resides in ∼24 kbyte of the 32 kbyte PROM. The system can be configured to load code from flash memory into SRAM and run it from there, supporting in-flight updates if necessary.
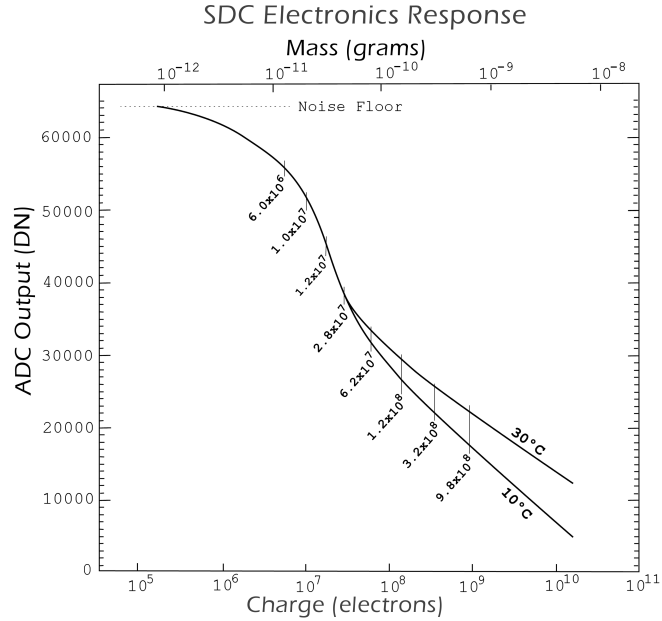
*Figure 5.* A typical SDC charge to DN response curve. Temperature dependent changes in gain are characterized during calibration. In-flight temperature monitoring and charge injection (the 8 onboard stimulus levels are indicated as vertical dashed lines) support post-processing correction for gain curve shifts.

3.4. SOFTWARE DESIGN

For most of the long journey to Pluto, the New Horizons payload will be in "hibernation", with the exception of SDC, which was designed for standalone operations. Much of the SDC flight software is related to managing itself during these long periods extending up to 500 days. In addition to data collection and storage, the software continuously executes a set of programmable 'autonomy' rules that allow the instrument to adjust for many off-nominal conditions.

When SDC is turned on it immediately starts taking science data. Ground commands are required only to perform calibrations or reconfigure settings. The ground can also turn channels off or on, erase the flash memory, and request telemetry packets. SDC provides several data packet types including science data, housekeeping information, calibration results, memory dumps, and message logs. Communications, as defined by the spacecraft, is limited to one command sent per second, and one telemetry packet received per second. A telemetry packet can contain up to 1024 data bytes.

### 3.4.1. *Data Management*

Whenever a science interrupt occurs the software compares each channel's value from the FPGA against that channel's current threshold value. For any channel exceeding its threshold the channel number, the measured value, and the threshold value are stored to flash memory along with the mission elapsed time (MET).

In addition to science data, flash memory is used for storing system housekeeping data and maintaining system critical variables, all of which are stored in triplicate. A simple majority vote is used to correct any corrupted values. A health check is performed on the flash memory everyday to ensure it can be written to and erased. Flight software maintains a table of ill-performing flash memory blocks.

### 3.4.2. *Autonomy Rules*

The 4 Mbyte of flash memory is much larger than the total expected SDC data volume. However, it is possible for elevated noise levels to be misidentified as science and potentially fill up the flash memory, leaving no room for real science. A high rate of noise events can also cause the software to hang while trying to process all the interrupts it receives. To mitigate the risk of filling-up flash memory during the long periods of unattended operation, the software has two sets of autonomy rules to control the data rate from the channels. Set A monitors the number of interrupts received from each channel every second. Whenever a channel generates 3 interrupts in a second (the maximum reasonable interrupt rate) that channel is blocked at the FPGA from generating further interrupts for some programmable period, typically one hour. These rules accommodate transient noise periods, like spacecraft maneuvers.

Set B monitors the number of interrupts received from each channel in a day. If a channel reaches the daily limit, by default 20, that channel's threshold is changed to a previously selected, less sensitive level. There is a table of three decreasingly sensitive threshold values for each channel, the values of which can be changed by ground command. The threshold of each channel can be increased twice, and if it remains in violation of Set B, then the channel is blocked from generating interrupts for a longer period, typically 30 days. After this time the channel is turned on at its original threshold and allowed to go through the table one more time. Upon reaching the end of the threshold table a second time the channel is permanently blocked from generating interrupts until enabled by ground command. The intent of this rule set is to autonomously adjust the instrument's sensitivity to permanent changes in the noise environment, such as degradation of the electronics. The time-out period of rule A and all of the rule B default values are adjustable by ground command.

### 3.4.3. *In-Flight Calibration Functions*

The flight software manages the setup and data collection of the Stimulus Test (3.3.2). In addition it can perform a Noise Floor calibration. This consists of temporarily suspending the autonomy rule set B and changing the thresholds of all the channels to a series of levels sensitive enough that electronics noise is detectable. By counting the number of science interrupts obtained at each threshold over specified times, the statistical distribution of the noise on each channel can be calculated. The flight software allows for up to five levels and test times. The test thresholds are configurable from the ground, but the durations are permanently set. At the completion of a test set, autonomy rule B is re-enabled and the channel thresholds are reset to their initial values.

### 3.5. INSTRUMENT CALIBRATION

### 3.5.1. *PVDF Sensor Characterization*

In the summer of 2003 and 2006 a set of SDC / PVDF sensors were taken to the dust accelerator facility at Max Planck Institute for Nuclear Physics in Heidelberg, Germany to verify that they show similar response to hypervelocity dust impacts (Figure 6) as has been published for previous instruments utilizing PVDF (Simpson and Tuzzolino, 1985).

More than 80 iron dust particle impacts where collected from 4 separate prototype sensors (Figure 7). At the lower particle sizes accurate measurements of CSA response was difficult. With these points excluded, the measured slope is close to that of Simpson and Tuzzolino (Eq. 1) but with an offset. This offset could be due to differences in the thickness of the metallic layers, their exact composition, and/or differences in the manufacturing of the PVDF, including its level of polarization. The fit to our calibration data (using the same notation as in Eq.1) is

$$N_e = 5.63 \times 10^{17} m[\mathrm{g}]^{1.3} v[\mathrm{km/s}]^{3.0}. \tag{2}$$

### 3.5.2. *Electronics Calibration*

The gain curve shown in Figure 5 illustrates that the system response to sensor produced charges is highly non-linear. A calibration function is needed to identify: a) the compression stage gain variation with electronics box temperature; and b) the possible change in CSA gain due to temperature driven changes in PVDF capacitance. The calibration equation then becomes $Q(\mathrm{DN}, \mathrm{T}_b, \mathrm{C}_{det}(\mathrm{T}_d))$, where Q in the measured charge, DN is the reported value, $\mathrm{T}_b$ is the temperature of the electronics box and $\mathrm{C}_{det}(\mathrm{T}_d)$ is the capacitance of the PVDF detector as a function of detector temperature, $T_d$.

PVDF detectors are very sensitive to acoustics and mechanical vibrations, making them impractical to use during calibration. From characterization
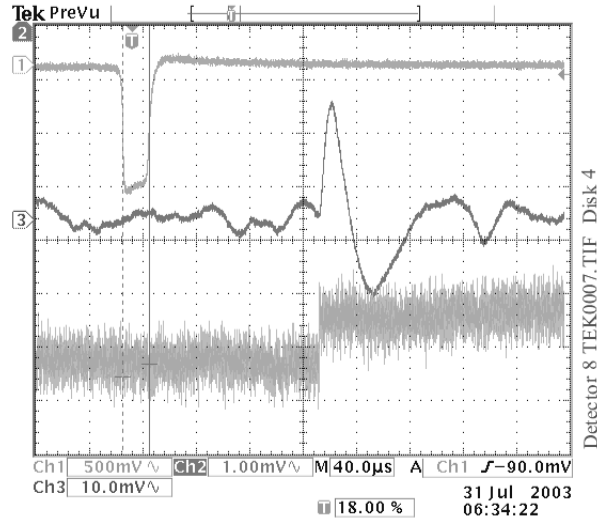
*Figure 6.* Example of output pulse from a PVDF sensor to a $3.1 \times 10^{-11}$ g iron particle impacting at 4.52 km/sec. The top trace is from the accelerator charge induction tube (100 mm, 6.1V/pC), the middle trace is the output of the shaper $(1.47 \times 10^{-5}$ mV/e) and the bottom trace is from the CSA $(7.3 \times 10^{-7}$ mV/e) (note: gains are not flight values).

of PVDF sensor capacitance over temperature, fixed capacitor values were selected to represent the detector capacitance, $C_{det}$, at 25, -30, and -100 °C. A range of reference charge pulses were generated with a standard calibrated charge injection circuit, and the electronics box temperature was collected from SDC telemetry points, measured at the shaper circuitry (the same measurements that are reported in flight). The measured electronics temperatures, $T_b$, were 50, 40, 34, and -7 °C.

For each electronics box temperature and $C_{det}$ value, 21 different amplitude charges were injected 100 times into each of the 14 channels. For each charge pulse injected the resulting DN value and accompanying $T_b$ were collected from the SDC telemetry. The pre-launch baseline calibration function for each channel, $Q_{ch}(DN, T_b)$, was produced by fitting that channel's data with a $10^{th}$ order polynomial. $C_{det}$ was dropped as a parameter to the calibration function after analysis showed that CSA gain changes due to variations in detector capacitance were insignificant.

## 4. Data analysis

When SDC data is received on Earth, it is sent to the New Horizons mission operations center at the Johns Hopkins University's Applied Physics Labora-
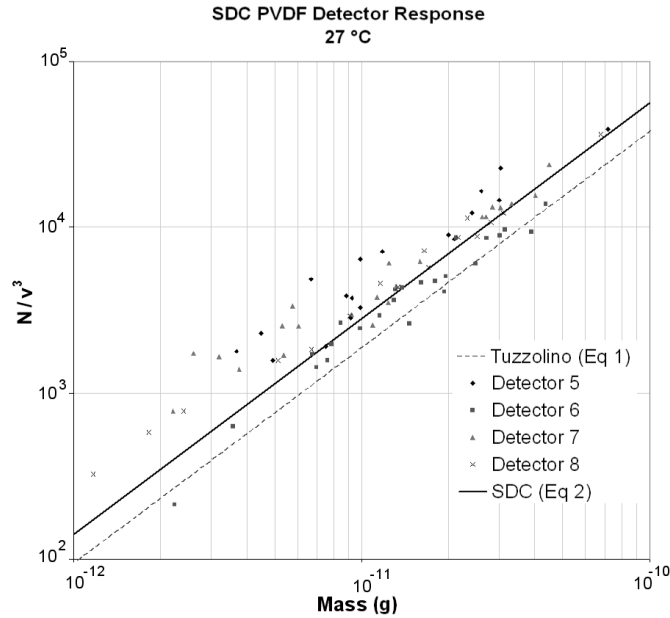
**SDC PVDF Detector Response**
**27 °C**



*Figure 7.* Dust impacts on SDC prototype PVDF sensors. Plot of ratio $N/v^3$ vs projectile mass. N (electrons) is the measured detector signal and v (km/s) is projectile velocity reported by the dust accelerator.

tory. The SDC data, as well as several ancillary spacecraft data packets, are also sent to SDCs home institution, LASP, via the Ground System Equipment Operating System (GSEOS). Simultaneously, it is also received at the Tombaugh Science Operations Center (TSOC) of the Southwest Research Institute (SwRI) in Boulder.

The data are sent through "levels" of processing software that progressively decode more of the packets and send the decoded data to the database.

− Level 0 software extracts the data packets out of the GSEOS files.

− Level 1 software separates the data by packet type, such as Science, Housekeeping, Calibration, flash and SRAM memory dumps, and decommutates the type specific data into the Level 1 database.

− Level 2 software generates charge values from Level 1 DN values using $Q_{ch}(DN, T_b)$ from section 3.5.2

− Level 3 software uses Eq. 2 to convert charge to equivalent mass

− Level 4 software removes noise using the reference detectors and other coincident events to produce validated IDP impact rates as function of dust mass.

The data products from Levels 0 through 2 are produced both at TSOC, as well as at LASP, using identical source controlled software. Data products from levels 3 and 4 are only produced at LASP.

## 5.  Initial results

### 5.1.  INITIAL TURN-ON AND CHECKOUT

On March 2, 2006, SDC was powered-on and commanded to report back a full set of housekeeping values. With receipt of fully nominal values, a series of commands were sent instructing the instrument to initiate a set of Stimulus Tests (ST) (section 3.3.2) and Noise Floor calibrations (NFC) (section 3.4.3). All tests ran successfully and the results showed that SDC had survived the rigors of launch. Both ST and NFC were repeated several times over the next few months to better characterize the post-launch behavior of the instrument.

### 5.2.  IN FLIGHT CALIBRATION

#### 5.2.1.  *Stimulus Calibration*
ST results were compared to pre-launch baseline tests. Figure 8 shows the change in stimulus responses for one of the channels. As of the time of the test, with the exception of channel 11, all of the stimulus test results were holding steady within the variation expected from ground testing. Some time between instrument delivery to the spacecraft and launch, the detector on channel 11 began exhibiting symptoms of degraded electrical contacts to the PVDF. As a result, channel 11 is expected to have a reduced sensitivity.

#### 5.2.2.  *Noise Floor Calibration*
With the sensitivity of the PVDF detectors to acoustics and mechanical vibrations, the in-flight NFC was the first good measure of SDC systematic noise. For each channel the average noise rate (noise events collected divided by collection period) versus threshold is calculated. The logarithm of the rates is used to fit a second degree polynomial to characterize the noise profile of that channel. The threshold value where the fit crosses the one hit per month rate, is the lowest of the three thresholds for that channel to support autonomy rule B (section 3.4.2). Figure 9 displays Noise Floor calibration data for a single channel and illustrates the threshold correction calculation.

A corrected set of thresholds were uploaded in late June 2006 and subsequently used for science collection through the fall. Two or three more rounds of calibrations are scheduled before entering cruise phase, during which the instrument must operate autonomously for up to 500 days.
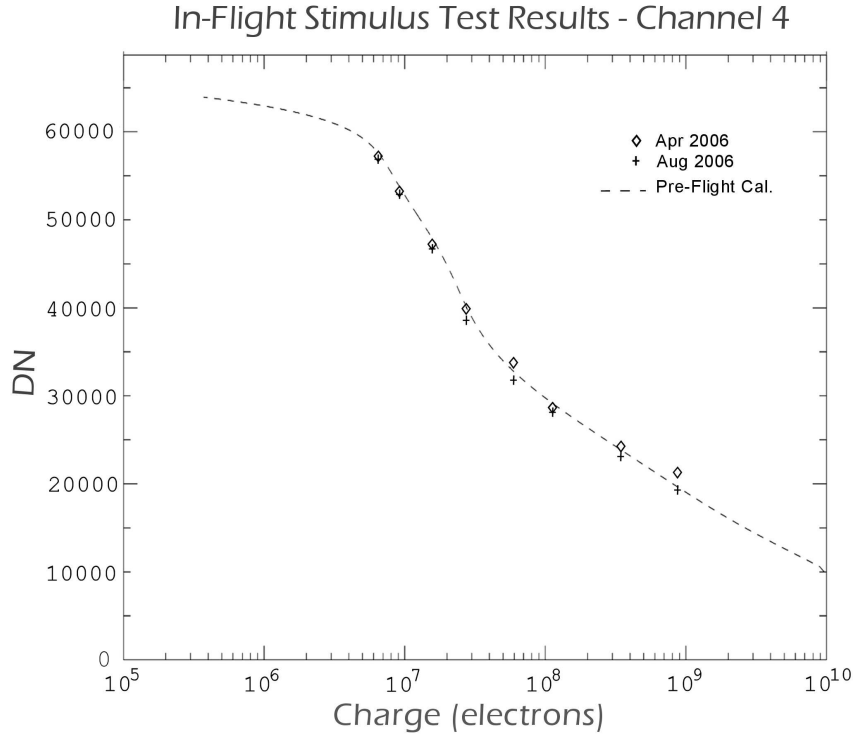
## In-Flight Stimulus Test Results - Channel 4



*Figure 8.* Stimulus tests of channel 4 performed in April and August, 2006, and the pre-flight calibration curve.

### 5.3. DUST MEASUREMENTS

SDC was designed to take advantage of the quiet state of the spacecraft during cruise phase. Various active spacecraft operations cause mechanical shocks that are picked up by the PVDF sensors and registered by SDC as science events. This is particularly true during three-axis pointing and active spin mode when the spacecraft frequently fires short bursts of the attitude thrusters. Level four data reduction (section 4) is used to filter out any hits that appear within a second of any thruster firing, thereby allowing science recovery between firings. However because the thruster induced events are often frequent enough to violate the autonomy rule B (section 3.4.2 ), during spacecraft maneuvers many SDC detector channels switch off for prolonged periods. During the first six months of flight, there are several periods, some weeks or months long, where SDC was completely off.

In spite of the initial difficulties of collecting science data, SDC does routinely take science during the short quiet periods available. As an exam-
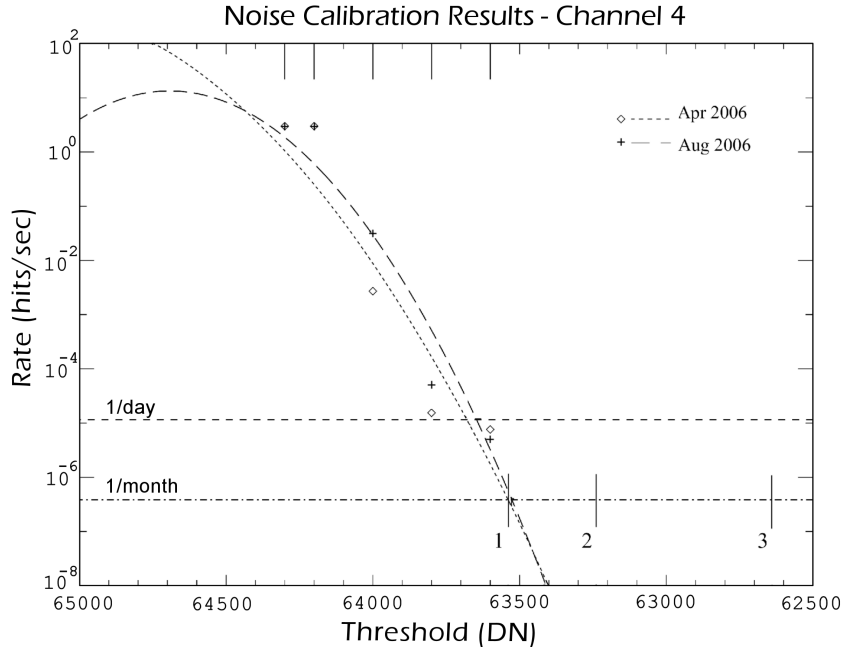
*Figure 9.* SDC channel 4 noise collected in April and August of 2006 using the Noise Floor calibration routine (section 3.4.3). The curves are fits to the collected rates at five separate thresholds (marked on the upper horizontal axis). The new science collection thresholds (lower vertical lines labeled 1, 2, and 3) are also indicated.

ple, Figure 10 shows the number of events recorded on each channel during segmented periods between July 14 and August 16, 2006, totaling 2.5 weeks. Events that were coincident between channels were removed, and channel 11 was excluded in this analysis. The average number of hits on the front sensors was 19.7±5.4, and on the reference sensors it was 18.0±4.2. The difference of these are taken to be real dust hits of 1.73±6.9 during this period, approximately consistent with our expectations of about 1 hit/week. The huge error bar is a consequence of the ongoing activities with other instruments on the spacecraft. Following the Jupiter encounter in February 2007, all other instruments will hibernate between scheduled yearly checkouts. SDC will stay on and start making measurements without interference.

## 6.  Conclusions

As part of the Education and Outreach effort of this mission, SDC provided a unique, hands-on opportunity for a group of undergraduate and graduate students to learn about building space hardware. Frequent 'all-hands'
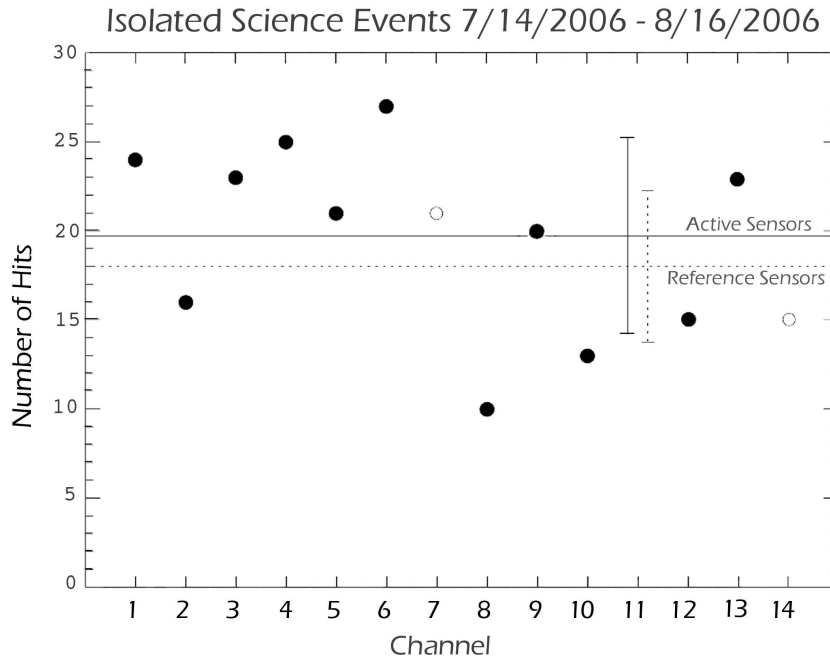
*Figure 10.* The number of single events registered on each of the SDC channels (with the exception of channel 11). These were recorded between 7/14/ 2006 and 8/15/2006, during a total operating period of about 2.5 weeks. The average number of hits and the $\pm 1\sigma$ error bars are also indicated for both the front (continuous line) and the reference (dashed line) sensors.

meetings during the development phases of SDC ensured that students and professionals working on all the subsystems (mechanical, thermal, analog and digital electronics, software, and operations) continuously discussed the requirements, as well as the schedule and the budget. SDC was delivered on time and within budget. A large fraction of the initial SDC students are pursuing careers in space research. During the next decade a smaller rotating group of students will operate the instrument and analyze our data. The SDC project was the first of its kind to be supported by EPO funds. Based on its history to date, it proved to be an excellent investment as part of the EPO effort of New Horizons.

In-flight tests, calibrations, and the initial science data show that SDC is performing according to expectations. It will continue to make measurements to improve our understanding of the spatial distribution of dust in the solar system. SDC will be the first dedicated instrument to measure dust impacts outside 18 AU, and it is expected to continue operating for the entire duration of the mission, deep inside the Kuiper Belt.

## Acknowledgements

## References

Bertolaccini, M. *et al.*: 1988, *Nuclear. Inst. Meth.*, **A264**, 399–406.

Divine, N.: 1993, *J. Geophys. Res.*, **98**, 17029–17051.

Grün, E. *et al.*: 1993, *Nature*, **362**, 428–430.

Humes, D. H.: 1980, *J. Geophys. Res.*, **85**, 5841–5852.

Jewitt, D.: 1999, *Annu. Rev. Earth. Planet. Sci.*, **27**, 287–312.

Liou, J. C., Zook, H. A., Dermott, S. F.: 1996, *Icarus*, **124**, 429–440.

Liou, J. C., Zook, H. A., Jackson, A. A.: 1999, *Icarus*, **141**, 13–28.

Liou, J. C., Zook, H. A.: 1999, *Astron. J.*, **118**, 580–590.

Moro-Martín, A., Malhotra, R.: 2002, *Astron. J.*, **124**, 2305–2321.

Moro-Martín, A., Malhotra, R.: 2003, *Astron. J.*, **124**, 2255-2265..

Radeka, V.: 1974, Signal, Noise and resolution in position-sensitive detectors. *IEEE Trans. Nucl. Sci.*, **NS-21**, 51–64.

Simpson, J.A., Rabinowitz, D., Tuzzolino, A. J.: 1989. *Nuclear Inst. Meth.*, **A279**, 611–624.

Simpson, J. A., Rabinowitz, D., Tuzzolino, A.J.: 1989, *Nuclear Inst. Meth.*, **A279**, 625–639.

Simpson, J. A., Tuzzolino, A. J.: 1985, *Nuclear Inst. Meth.*, **A236**, 187–202.

Spieler, H.: 2005, *Semiconductor Detector Systems.* Oxford University Press, New York U.S.A, ISBN-0-19-852784-5

Srama, R. *et al.*: 2004, *Space Sci. Rev.*, **114**, 465–518.

Stern, A.: 1996, *Astron. Astrophys.*, **310**, 999–1010.

Tuzzolino, A. J.: 1983, *Nuclear Inst. Meth.*, **212**, 505–516.

Tuzzolino, A. J.: 1992, *Nuclear Inst. Meth.*, **A316**, 223–237.

Tuzzolino, A. J.: 1996, *Adv. Space Res.*, **17**, 123–131.

Tuzzolino, A.J., McKibben, R.B., Simpson, J.A., BenZvi, S., Voss, H.D., Gursky, H.: 2001, *Planetary and Space. Sci.*, **49**, 689-703.

Tuzzolino, A. J., *et al.*: 2003, *JGR*, **108**, doi: 10.1029/2003JE002086.